A COMPARISON BETWEEN LINEAR AND NON-LINEAR SPECTRAL UNMIXING METHODS

Ahmed, Asmau Mukhtar
Department of Geography,
Kaduna State University

Abstract
Spectral unmixing is a key process in identifying the spectral signature of materials and quantifying their spatial distribution over an image. This paper aims to investigate linear and nonlinear methods used to solve spectral unmixing problems, the methods were compared based on their prediction accuracy, robustness against noise and computational time using laboratory simulated data. Results show that the nonlinear methods outperform the linear methods in terms of prediction accuracy and robustness against noise but are computationally more expensive.

Keywords: Spectral Unmixing, Hyperspectral Image, Linear Mixing Model, Nonlinear Mixing Model,

INTRODUCTION

Spectral Unmixing (SU) is the process of identifying spectral signatures of materials often referred to as endmembers and also estimates their relative abundance to the measured spectra (Keshava and Mustard, 2002). It involves the analysis of hyperspectral/multispectral data in different fields of application such as remote sensing, planetary science, material science and mineralogy (Dobigeon, 2014). Spectral unmixing often requires the definition of the mixing model underlying the observations as presented in the data. A mixing model describes how the endmembers combine to form the mixed spectrum as measured by the sensor (Hapke, 1981). Given the mixing model, SU then estimates the inverse of the formation process to infer the quantity of interest, specifically the endmembers, and abundance from the collected spectra (Dobigeon, 2014). This could be achieved through a radiative transfer model which accurately describes the light scattering by the materials in the observed scene by a sensor as shown in Figure 1.

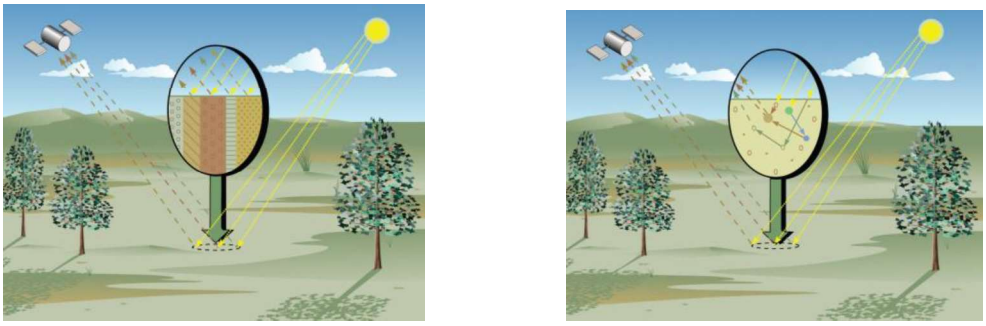

(a) (b)

Figure 1: Two mixing models. (a) The linear mixing model assumes a well-defined checker board mixture of materials, with a single reflection of the illuminating solar radiation. (b) Nonlinear mixing models assume a randomly distributed, homogeneous mixture of materials, with multiple reflections of the illuminating radiation. (Adopted from Hapke, 1981)

A hyperspectral image consists of spatial and spectral dimensions which correspond to the different wavelengths at which the scene is observed (Yoann, 2013). The hyperspectral image is often in the form of reflectance, that is the vector of values associated with each pixel is the reflectance vector or spectrum of the corresponding surface in the scene.

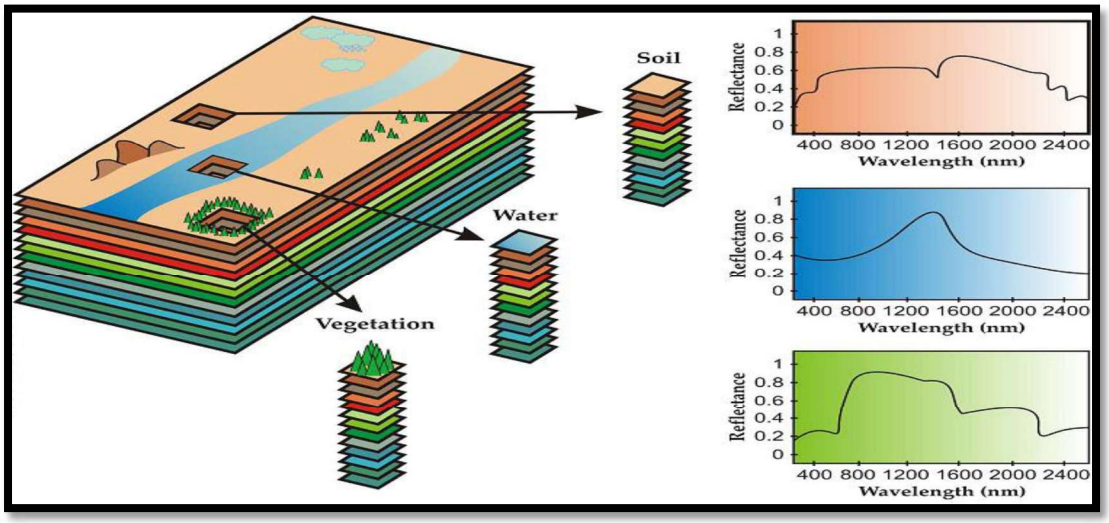

Figure 2: Concept of HyperspectralImage (Adopted from Gillespie et al., 1990)

This spectrum is composed of different materials such as water, soil, vegetation etc which are often referred to as endmembers as shown in Figure 2. An important problem in hyperspectral imaging processing is to decompose the mixed pixels

into the materials that contribute to the pixel, endmembers and the corresponding fractions of the spectral signatures in the pixel. This is often referred to as the unmixing problem (Gillespie et al., 1990).
When the mixing scale formed in the scene is macroscopic and each photon reaching the sensor interacted with only one material, then the measured spectrum $y_p \in R^L$ in the p_{th} pixel can be accurately described by the Linear Mixing Model (LMM) (Dobigeon, 2014).

Linear Spectral Unmixing Model
The linear unmixing model was first proposed by (Harold et al., 1996) who made the assumption that there is no multiple scattering between different cover types; it was believed that each photon interact with a single cover type as shown in (Figure 1). Linear unmixing is widely used in the spectral unmixing process. When the endmembers and spectral reflectances are known, the linear mixing model is then used to estimate their abundances in each pixel and be solved using equation 1 (Duran and Petrou, 2004).

Equation 1. $$y_p = \sum_{r=1}^{R} a_{rp} m_r + n_p \quad \text{.....(1)}$$

Where $\boldsymbol{R}$ is the number of endmembers present in the image, $\boldsymbol{m_r}$ is the spectral signature of the $\boldsymbol{r^{th}}$ endmember, $\boldsymbol{a_{rp}}$ is the abundance of the $\boldsymbol{r^{th}}$ material in the $\boldsymbol{p^{th}}$ pixel and $\boldsymbol{n_p}$ is an additive noise and modeling error.

Nonlinear Unmixing Method
Due to the simplicity of the linear mixing model, they have been widely used for hyperspectral image analysis. However, several studies have noted that the linear mixing model can be inaccuratein particular situations (Bioucas-Dias et al., 2012), because they fail to in-cooperate back scatter radiation, in this case, more complex models must be adopted to solve the unmixing problem. Nonlinear mixing models cope with nonlinear interactions; they capture the nonlinear effects that are mostly present in an image (Dobigeon, 2014).

When interactions occur at a microscopic level, it is said that the materials are intimately mixed, for example, this scene is an area that is composed of sand or mineral mixtures (Figure 1). A model described by (Hapke, 1981) describes the interactions suffered by light when it comes to contact with surface a composed of particles; they involve meaningful and interpretable quantities that have physical significance, however, these models require a nonlinear formulation which is

complex and complicates the derivation of the unmixing strategies (Dobigeon, 2014). In Hapke (1981), the authors derived an analytical model used to express the measured reflectances as a function of parameters intrinsic to the mixtures, these include massfraction, density size and single scattering albedo, however, this model's limitation is that it depends solely on parameters inherent to the experiment because it requires the full information of the geometric position of the sensor with respect to the observed samples therefore making the inversion process more challenging to implement especially when the spectral signatures of the endmembers are unknown (Keshava and Mustard, 2002).

MODELS USED FOR THE COMPARISON

The models used for the comparisonincluded;Vertex Component Analysis (VCA) and Minimum Volume Simplex Analysis (MVSA)for the linear models and the Generalised Bilinear Model (GBM) and the Polynomial Post Nonlinear Mixing Model (PPNMM) were usedfor the nonlinear model. VCA was chosen because it is a model that assumes the presence of at least one pure pixel in an image while MVSA does not, in this case, we want to know which model performs best in terms of unmixing a hyperspectral data with at least 3 endmembers. The GBM was considered because the model addresses multiple scattering effects and assumes the presence of multiple photon interaction by introducing additional interaction terms to cope with the nonlinear effect while the PPNMM is a flexible nonlinear model that detects nonlinearity in an image pixel and relates the endmembers on an image by a polynomial.

Vertex Component Analysis (VCA)

This algorithm is based on the geometry of convex sets; it exploits the fact that endmembers occupy the vertices of a simplex (Nascimento & Dias, 2005a). The VCA algorithm assumes the presence of spectrally pure pixels in a dataset and iteratively projects the data onto the direction orthogonal to the subspace spanned by the end members that are already determined (Arthur, 1996). The new endmember signature corresponds to the extreme of the projection. The algorithm iterates until all endmembers are exhausted (Bioucas-Dias et al., 2012).

Minimum Volume Simplex Analysis (MVSA)

This algorithm belongs to the minimum volume class and is able to unmix a hyperspectral data set in which the pure pixel assumption is not fulfilled (Li & Bioucas-Dias, 2008). MVSA is initialized with an inflated version of the simplex provided by the VCA (Nascimento & Dias, 2005b), then MVSA removes the positivity hard constraint for the abundance fractions and uses instead a step

designed to make the algorithm robust against outliers (Duran & Petrou, 2011). On the other hand does not assume the presence of pure pixels in an image, like the VCA algorithm, the MVSA algorithm is also unsupervised, it belongs to the minimum volume class, and this is able to unmix hyperspectral data set in which the pure pixel assumption is not fulfilled (Li &Bioucas-Dias, 2008). MVSA is initialized with an inflated version of the simplex provided by VCA (Nascimento & Dias, 2005a), then MVSA removes the positivity hard constraint for the abundance fractions and uses instead a step designed to make the algorithm robust against outliers (Duran & Petrou, 2011).

Generalized Bilinear Mixing Models (GBMM)

This methodaccounts for the presence of multiple photon interactions by introducing additional interaction terms in the linear mixing model as detailed in equation 2(Somers et al., 2009). The bilinear model considers second order interactions between endmembers $\neq i \; and \; \neq j \; (for \; i,j = 1, \ldots., R \; and \; i \; \neq j)$ such that the observed mixed pixel y can be written as

Equation 2

$$\mathrm{y}_p = \sum_{r=1}^{R} a_{r,p}\mathrm{m}_r + \sum_{i=1}^{R-1}\sum_{j=i+1}^{R} \gamma_{i,j,p} a_{i,p} a_{j,p} \mathrm{m}_i \odot \mathrm{m}_j + \mathrm{n}_p,$$

Where $\odot$ is the Hadamard (term by term) product operation. GBMM reduces the additivity constraints imposed on the abundances by the linear mixing model. The Generalized Bilinear model, unlike the other family of bilinear mixing models such as the Nascimento and Fan bilinear models, assumes that the contribution of the interaction term $\boldsymbol{mi} \odot \boldsymbol{mj}$ is proportional to the fractions of the involved components with amplitude $\gamma_{ij}\alpha_i\alpha_j$. The additional parameter γ_{ij} introduced in the GBMM is to obtain a more flexible model as compared to the Nascimento and Fan models. The GBMM can be performed using the Bayesian algorithm or the least square methods to estimate the unknown parameters (Altmann et al., 2011;, Altmann et al., 2012).

Polynomial Post Nonlinear Mixing Model (PPNMM)

This model assumes that the reflectance of an image isa nonlinear function of pure spectral components contaminated by additive noise; the nonlinear functions are often approximated using a polynomial function leading to a polynomial post-nonlinear mixing model as detailed in equation 3 (Duran & Petrou, 2011).

The model involves linear and quadratic functions of the abundances. In this case, the L-spectrum Y= [$y_1, \ldots, y_L$] of a mixed pixel is defined as a nonlinear transformation g of a linear mixture of R spectra m_r contaminated by additive noise as shown in equation 3.

Equation 3

$$\mathbf{y}_p = \mathbf{g}_p \left(\sum_{r=1}^{R} a_{r,p} \mathbf{m}_r \right) + \mathbf{n}_p$$

where m_r is the spectrum of the r^{th} material in the scene,a_r its corresponding proportion, R is the number of endmembers contained in the image and g is an appropriate nonlinear function. Another motivation for the PPNMM is the Weierstrass approximation theorem which states that every continuous function defined on an interval can be uniformly approximated by a polynomial with any desired precision (Altmann, et al., 2011).

All four methods were compared on synthetic data based on performance concerning the quality of the unmixing method and computational time. The quality of the unmixing method for synthetic images can be measured by comparing the estimated and the actual abundances by using the Root Mean Square Error (RMSE) (Altmann et al., 2012) thus the lower the RMSE the better the result.

DATA DESCRIPTION

The simulated data used for the comparison was obtainedfrom (Li & Bioucas-Dias, 2008). The data has a size n = 10000 pixels and 3 endmembers (Carnallite, Ammonioalunite and Biotite) as shown in Figures 3, 4 and 5, the dataset was generated according to the linear observation model, the abundance fractions are Dirichlet distributed with parameters μ = 1 for i = 1,...p, the spectral signatures of the endmembers are mineral reflectance with 224 bands obtained from the ENVI spectral library. Figure 3, 4 and 5 shows the spectral signatures of the true and estimated signatures. For the nonlinear methods, the same data was then generated with an abundance vector of a_1 = 0.3, a_2 = 0.6 and a_3 = 0.1, a nonlinearity coefficient was uniformly generated in the set [0,1], the PPNMM parameter p = 1 was generated uniformly in the set [-0.3, 0.3], the image was corrupted with Random Gaussian noise of varianceσ^2 = 2.8 * (10^{-3}) which is equivalent to a Signal to Noise Ratio (SNR) 30dB. Simulation was conducted on the data with different levels of Signal to Noise Ratio ranging between (SNR) 10dB and (SNR) 50dB. This is to ascertain the robustness of the methods with regard to the high

signal-to-noise ratio, each result is based on 100 runs. The result of the unmixing based on RMSE of the four methods is presented in Table 1

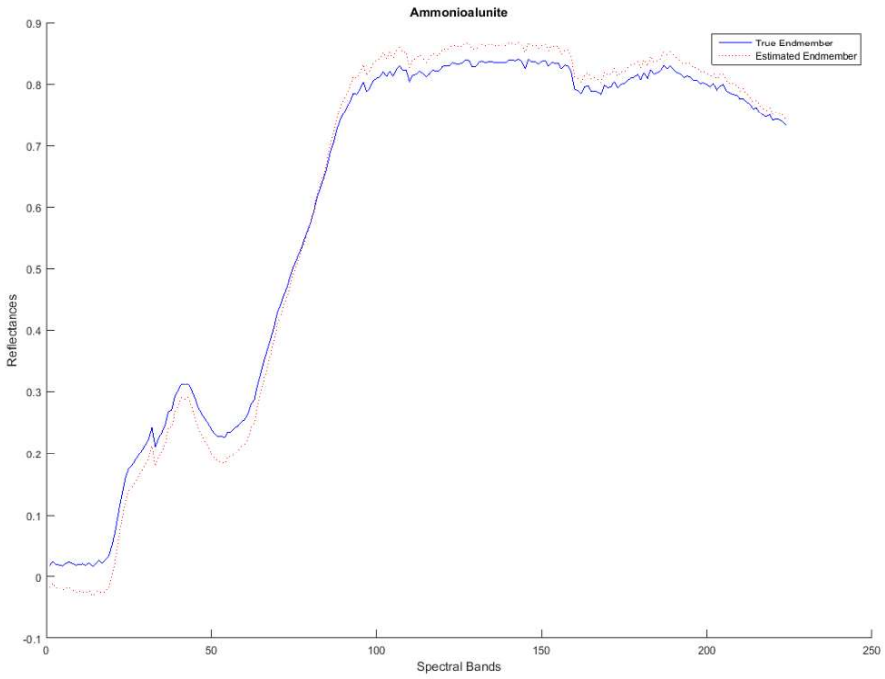

Figure 3 Spectral reflectance of Ammonialunite endmember

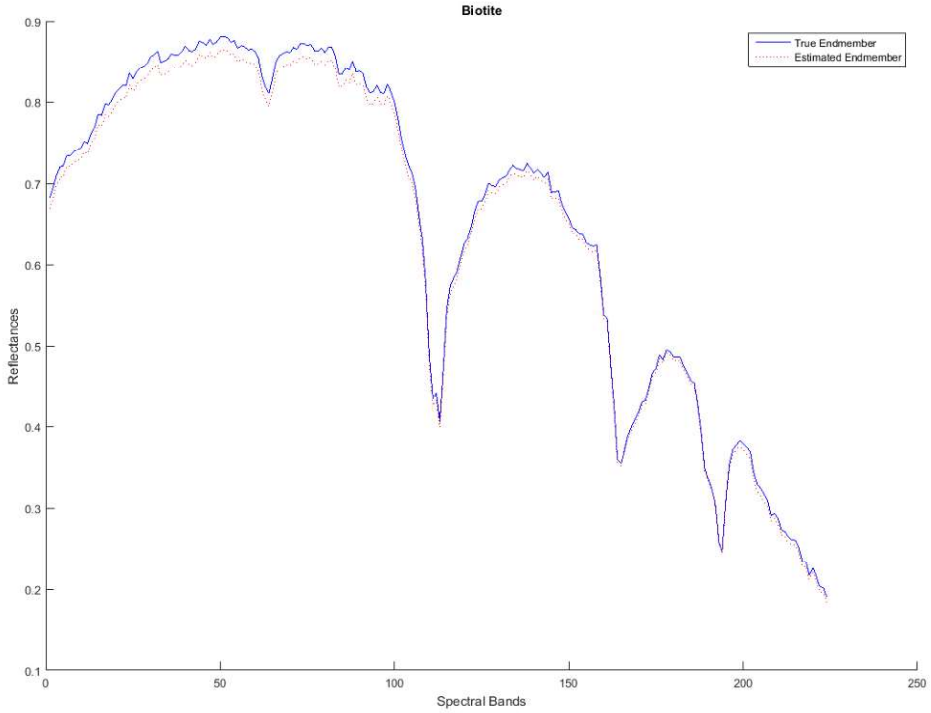

Figure 4 Spectral reflectance of Biotite endmember

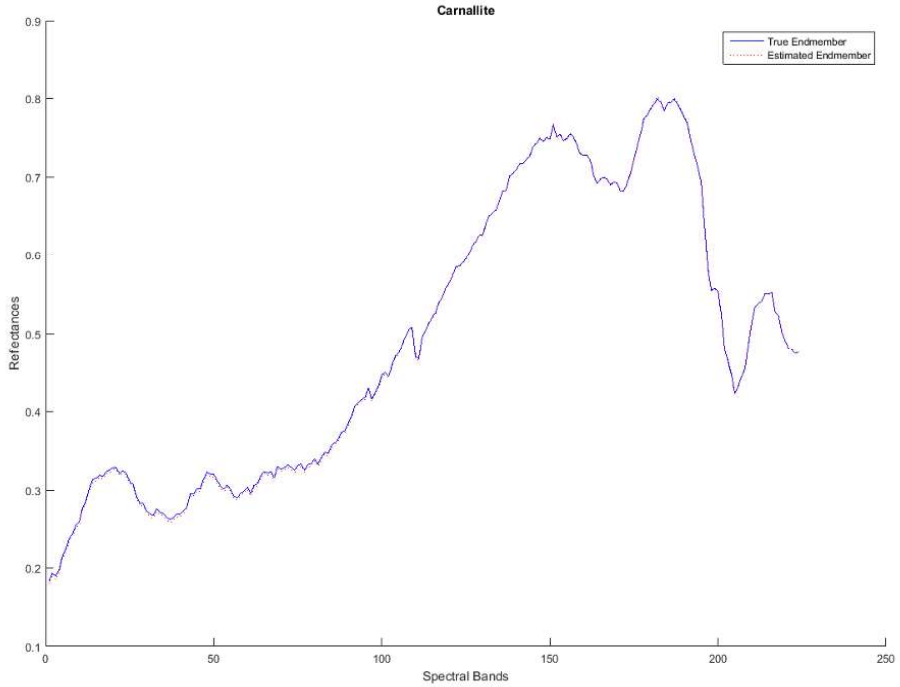

Figure 5 Spectral reflectance of Carnalite endmember

SIMULATION RESULTS

Table 1shows the comparison of the four methods on simulated data showing the Root mean square error (RMSE) and Computational Time (C.T) in seconds for the four algorithms with different Signal to Noise Ratio (SNR)

Table 1:Comparison of the four spectral unmixing methods on simulated data

ALGORITHM	SNR=10dB	C.T (sec)	SNR=30dB	C.T (sec)	SNR=50dB	C.T (sec)
VCA	0.1933	0.110	0.0952	0.120	0.0808	0.110
MVSA	0.1804	0.550	0.0096	0.500	0.0028	0.990
GBM	3.1126(*10^{-2})	1.678	2.7233(*10^{-2})	1.431	2.500(*10^{-2})	1.130
PPMM	4.333(*10^{-2})	1.254	3.706(*10^{-2})	1.101	3.005(*10^{-2})	1.100

Source: (Author 2023)

DISCUSSION

Two models each of linear and nonlinear methods were compared based on the quality of the unmixing model on synthetic data and computational time. The simulation result was conducted on an LG desktop with processor: intel (R) core TM^2 Duo CPU 3.00 GHZ. Results of the experiment reveal that the nonlinear methods outperform the linear models with lower root mean square error even in the presence of a high signal-to-noise ratio as shown in (Table 1) but in turn are computationally expensive when compared with the linear models, this could be because the nonlinear models detect nonlinearity in a data and also account for backscatter radiation. However the linear models performed better with a low signal-to-noise ratio which shows a similar result (Duran & Petrou, 2011), therefore this result can further be expanded into hybridization between the linear and nonlinear models with regards to signal-to-noise ratio.

CONCLUSION

From the results obtained, it has been demonstrated thatthe nonlinear models are better in spectral unmixing of hyperspectral data with a high Signal to Noise Ratio and the linear models are better when the Signal to Noise Ratio is lower at a certain ratio. This will be investigated by conducting a hybridization of the two models.

REFERENCES

Altmann, Y., Halimi, A., Dobigeon, N., & Tourneret, J. Y. (2011, May). Supervised nonlinear spectral unmixing using a polynomial post nonlinear model for hyperspectral imagery. In *2011 IEEE International Conference on Acoustics, Speech and Signal Processing (ICASSP):* (1009-1012). IEEE.

Altmann, Y., Halimi, A., Dobigeon, N., & Tourneret, J. Y. (2012). Supervised nonlinear spectral unmixing using a postnonlinear mixing model for hyperspectral imagery. *IEEE Transactions on Image Processing*, 21(6):;- 3017-3025.

Arthur, W. R. (1996). Fundamentals of electronic image processing. *Fundamentals of Electronic Image Processing*.

Bioucas-Dias, J. M., Plaza, A., Dobigeon, N., Parente, M., Du, Q., Gader, P., & Chanussot, J.

(2012). Hyperspectral unmixing overview: Geometrical, statistical, and sparse regression-based approaches. *IEEE journal of selected topics in applied earth observations and remote sensing*, 5(2):,- 354-379.

Dobigeon, N., Tourneret, J. Y., Richard, C., Bermudez, J. C. M., McLaughlin, S., & Hero, A. O. (2013). Nonlinear unmixing of hyperspectral images: Models and algorithms. *IEEE Signal processing magazine*, 31(1):, 82-94.

Duran, O., & Petrou, M. (2010). Robust endmember extraction in the presence of anomalies. *IEEE Transactions on Geoscience and Remote Sensing*, 49(6):, 1986-1996.

Duran, O., & Petrous, M. (2004). Mixed pixel classification in remote sensing—literature survey. *School of Electronics and Physical Sciences, University of Surrey: Guildford, UK*.

Duran, O., & Petrou, M. (2010). Robust endmember extraction in the presence of anomalies. *IEEE Transactions on Geoscience and Remote Sensing*, 49(6):, 1986-1996.

Gillespie, A. R. (1990). Interpretation of residual images: spectral mixture analysis of AVIRIS images, Owens Valley, California. In *Proc. second airborne visible/infrared imaging spectrometer (AVIRIS) workshop*:-(243-270). Jet Propulsion Laboratory.

Hapke, B. (1981). Bidirectional reflectance spectroscopy: 1. Theory. *Journal of Geophysical Research: Solid Earth*, 86(B4):, 3039-3054.

Horwitz, H. M., Nalepka, R. F., Hyde, P. D., & Morgenstern, J. P. (1971, January). Estimating the proportions of objects within a single resolution element of a multispectral scanner. In *International Symposium on Remote Sensing of Environment, 7th, University of Michigan*.

Keshava, N., & Mustard, J. F. (2002). Spectral unmixing. *IEEE signal processing magazine*, 19(1):, 44-57.

Li, J., & Bioucas-Dias, J. M. (2008, July). Minimum volume simplex analysis: A fast algorithm
to unmix hyperspectral data. In *IGARSS 2008-2008 IEEE International Geoscience and*
*Remote Sensing Symposium,*3:III-250
Nascimento, J. M., & Dias, J. M. (2005a). Vertex component analysis: A fast algorithm to unmix
hyperspectral data. *IEEE transactions on Geoscience and Remote Sensing*, 43(4):, 898-
910.
Nascimento, J. M., & Dias, J. M. (2005b). Does independent component analysis play a role in
unmixing hyperspectral data?. *IEEE Transactions on Geoscience and Remote*
Sensing, *43*(1):, 175-187.
Somers, B., Cools, K., Delalieux, S., Stuckens, J., Van der Zande, D., Verstraeten, W. W., &
Coppin, P. (2009). Nonlinear hyperspectral mixture analysis for tree cover estimates in
orchards. *Remote Sensing of Environment*, *113*(6):, 1183-1193.
Yoann Altmann. (2013). Nonlinear spectral unmixing of hyperspectral images. PhD thesis,
lnstitute National Polytechnique de Toulouse (INP Toulouse), October 2013.